Histologic Development of the Human Fovea From Midgestation to Maturity

ANITA HENDRICKSON, DANIEL POSSIN, LEJLA VAJZOVIC, AND CYNTHIA A. TOTH

Purpose: To describe the histologic development of the human central retina from fetal week (Fwk) 22 to 13 years.

• DESIGN: Retrospective observational case series.

• METHODS: Retinal layers and neuronal substructures were delineated on foveal sections of fixed tissue stained in azure II–methylene blue and on frozen sections immunolabeled for cone, rod, or glial proteins. Postmortem tissue was from 11 eyes at Fwk 20–27; 8 eyes at Fwk 28–37; 6 eyes at postnatal 1 day to 6 weeks; 3 eyes at 9 to 15 months; and 5 eyes at 28 months to 13 years.

• RESULTS: At Fwk 20–22 the fovea could be identified by the presence of a single layer of cones in the outer nuclear layer. Immunolabeling detected synaptic proteins, cone and rod opsins, and Müller glial processes separating the photoreceptors. The foveal pit appeared at Fwk 25, involving progressive peripheral displacement of ganglion cell, inner plexiform, and inner nuclear layers. The pit became wider and shallower after birth, and appeared mature by 15 months. Between Fwk 25 and Fwk 38, all photoreceptors developed more distinct inner and outer segments, but these were longer on peripheral than foveal cones. After birth the foveal outer nuclear layer became much thicker as cone packing occurred. Cone packing and neuronal migration during pit formation combined to form long central photoreceptor axons, which changed the outer plexiform layer from a thin sheet of synaptic pedicles into the thickest layer in the central retina by 15 months. Foveal inner and outer segment length matched peripheral cones by 15 months and was 4 times longer by 13 years.

• CONCLUSIONS: These data are necessary to understand the marked changes in human retina from late gestation to early adulthood. They provide qualitative and quantitative morphologic information required to interpret the changes in hyper- and hyporeflexive bands in pediatric spectral-domain optical coherence tomography images at the same ages. (Am J Ophthalmol 2012; 154:767–778. © 2012 by Elsevier Inc. All rights reserved.)

See Accompanying Article on page 779.

Accepted for publication May 8, 2012.

From the Departments of Ophthalmology (A.H., D.P.) and Biological Structure (A.H.), University of Washington, Seattle, Washington; Department of Ophthalmology, Duke University Eye Center (L.V., C.T.), Durham, North Carolina; and Department of Biomedical Engineering, Pratt School of Engineering (C.T.), Duke University, Durham, North Carolina.

Inquiries to Cynthia A. Toth, Duke Eye Center, Box 3802, 2351 Erwin Rd, Suite 103, Durham, NC 27710; e-mail: cynthia.toth@duke.edu

THE FOVEA IS THE MOST CRITICAL PORTION OF THE primate retina for high visual acuity and color vision. Its early development begins at fetal week (Fwk) 12 with a complex expression sequence of cell-specific molecules.[1–7] After midgestation an outward displacement of inner retinal layers occurs to form a foveal pit, and after birth an inward displacement of the photoreceptors occurs to raise foveal cone density 10×.[8–17] Spectral-domain optical coherence tomography (SDOCT) has become a valuable tool for clinical diagnosis of normal and diseased adult human retina.[18] Recently, Maldonado and associates[19] used a portable research hand-held SDOCT unit to image human retinas from premature infants through adults. They documented the immaturity of the neonatal human fovea and the marked difference in SDOCT layers from the standard adult SDOCT image. However, there is still little detailed description of histologic development and almost no quantitative information about human central retina around birth. This paper provides the first detailed histologic description of human central retinal development from midgestation to early adulthood. In particular, it shows the marked change in foveal photoreceptors from a single layer of short undeveloped cones up to birth to tightly packed and highly elongated cones in the adult. Understanding these changes is essential to make the correct interpretation of neonatal SDOCT images.

METHODS

TISSUE SECTIONS FOR THIS STUDY WERE FROM EYES OBtained under Human Subjects Approval #010447. Eyes younger than Fwk 22 were from elective abortions; only normal-appearing fetuses were used. Older prenatal and neonatal eyes were from infants who survived days to weeks in the neonatal intensive care unit; babies with diagnosed conditions that might affect retinal development were not included in this report. Infant eyes were obtained from children who died of accidental causes, or of diseases that did not affect the retina.

Eyes were enucleated 2–8 hours after death, the cornea and lens removed, and the globe immersed in a mixture of 4% paraformaldehyde and 0.5% glutaraldehyde in pH7.4 phosphate buffer (PB) for 1 day to months. In 1 of the pair of eyes, the horizontal meridian was embedded in glycol methacrylate and cut serially at 2–3 μm. This method

0002-9394/$36.00
http://dx.doi.org/10.1016/j.ajo.2012.05.007
© 2012 BY ELSEVIER INC. ALL RIGHTS RESERVED.

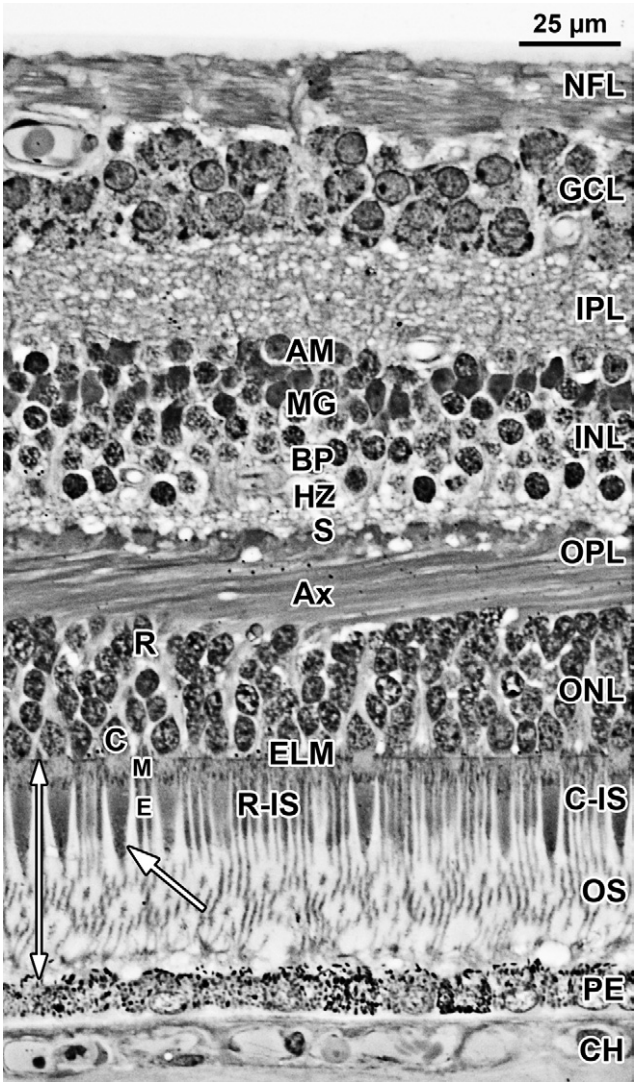

FIGURE 1. Layers and histology of normal adult human retina. Adult human retina 2 mm nasal from the fovea center. The layers and their abbreviations used in this paper and in subsequent figures are choroid (CH); retinal pigment epithelium (PE); outer nuclear layer (ONL), which is subdivided into the photoreceptor outer segment (OS) and inner segment (IS) layers distal to the external limiting membrane (ELM); and the nuclear layer containing a single row of cone (C) cell bodies near the ELM and multiple rows of deeper rod (R) cell bodies. The thin rod IS are indicated (R-IS). The rod OS are about half the thickness of the rod IS, are longer and reach the PE. The larger tapered cone IS have a shorter OS (arrow). The ELM marks the distal edge of the retina. IS myeloid (M) and ellipsoid (E) are indicated. The outer plexiform layer (OPL) contains a distal layer made up of the fibers of Henle or photoreceptor axons (Ax) and a proximal synaptic contact layer (S) containing cone pedicles and rod spherules. The inner nuclear layer (INL) contains the cell bodies of horizontal cells (HZ) lying most distal, bipolar cells (BP) in the middle, Müller glia (MG), and amacrine cells (AM) lying most proximal. The inner plexiform (IPL), ganglion cell (GCL), and nerve fiber (NFL) layers complete the inner retina.

gives excellent preservation and imaging of tissue. In a few eyes the entire globe was embedded in paraffin and sectioned serially at 12 µm. This method was less time-consuming, but the retina was usually detached from the pigment epithelium. In some eyes the horizontal meridian was frozen-sectioned serially at 12 µm, allowing immunolabeling at a known locus with a wide variety of antibodies. In each method, every tenth slide was stained with 1% azure II–methylene blue to locate the fovea.

• **IMMUNOLABELING:** Frozen sections were labeled as previously reported.[5,7] The rod marker was mouse anti-rod opsin (4D2, 1/300; gift of R. Molday). Cone markers included rabbit anti-long-and-medium (L&M)-wavelength-selective cone opsin (1/2000, gift of J. Saari), rabbit anti-short (S)-wavelength-selective cone opsin (1/10 000, gift of J. Nathans), mouse anti-cone arrestin (7G6, 1/250–500; gift of P. MacLeish), and mouse anti-cone alpha transducin (A1.1, 1/250–500; gift of J. Hurley). Mouse anti-synaptophysin (1/1000; Sigma-Aldrich S5768) labels cone synaptic pedicles heavily and rod synaptic spherules lightly. Rabbit anti–cellular retinaldehyde-binding protein (CRALBP; 1/1000; gift of J. Saari) was used to label Müller glial cytoplasm.

• **IMAGING:** All photographs were from sections in which the foveal center could be reliably identified. Plastic or paraffin sections stained with azure II–methylene blue were imaged digitally using a Nikon E1000 wide-field digital microscope (Nikon Instruments, Inc, Melville, New York, USA). Immunolabeled sections were imaged using a high-sensitivity Hamamatsu camera (Hamamatsu Corp, Bridgewater, New Jersey, USA) or in an Olympus Fluoview 1000 confocal microscope (Olympus America, Center Valley, Pennsylvania, USA). All images were processed in Adobe Photoshop CS5 for size, color balance, sharpness, and contrast.

• **SEGMENTATION OF LIGHT MICROGRAPHS:** A low-power foveal montage was created at selected ages. One half was imaged in Photoshop and paths drawn along the inner surface of the retina and the borders between the ganglion cell (GCL) and inner plexiform layer (IPL); the IPL and inner nuclear layer (INL); the INL and outer plexiform layer (OPL); the OPL and outer nuclear layer (ONL); and the inner border of the retinal pigment epithelium (RPE). Layers were differentially shaded ((Figure 1 provides an orientation to the layers; Figures 2 through 7 show shaded layers).). In young retinas, the OPL was thin and included in ONL, but in older retinas the OPL was distinguished as a separate layer. A dotted path was drawn along the external limiting membrane (ELM), separating the proximal ONL from the distal inner segment/outer segment (IS/OS) layer.

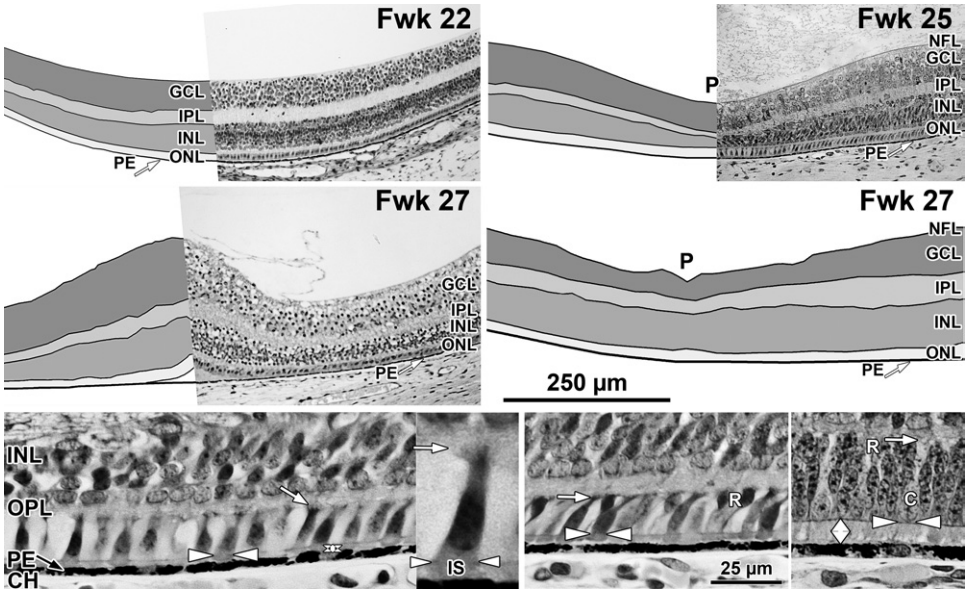

FIGURE 2. Layers and histology of midgestation fetal human retina. Development of the human fovea at (Top left) fetal week (Fwk) 22, (Top right) Fwk 25, and (Middle left and right) Fwk 27. Retinal layers have been drawn from digital photographs using Adobe Photoshop (see Methods) and the layers shaded as indicated. (Top left) At Fwk 22 the foveal region is composed of 5 layers with a thick GCL and a thin ONL. (Top right, Middle right) After Fwk 25 the foveal pit (P) begins to invaginate the inner retinal layers. (Bottom left) At Fwk 25 there is only a very narrow space (vertical double arrow) between the ELM (horizontal white arrowheads) and the PE in central retina. The cone marked with arrowheads is shown at higher power in the inset to the right. A short thick IS extends distal to the ELM (white arrowheads) and a small synaptic pedicle (arrow) is present. (Bottom middle) At 800 µm from the fovea there is little difference from the fovea except that 2 rods (R) are present. (Bottom right) At 2 mm from the fovea a slightly wider PE/ELM space is present (vertical double arrow) and is filled with cone and rod IS. OS are not obvious. Scale in Middle right for Top and Middle rows; in Bottom middle for Bottom row. C = cone; CH = choroid; ELM = external limiting membrane; GCL = ganglion cell layer; INL = inner nuclear layer; IPL = inner plexiform layer; IS = inner segment; NFL = nerve fiber layer; ONL = outer nuclear layer; OPL = outer plexiform layer; PE =retinal pigment epithelium.

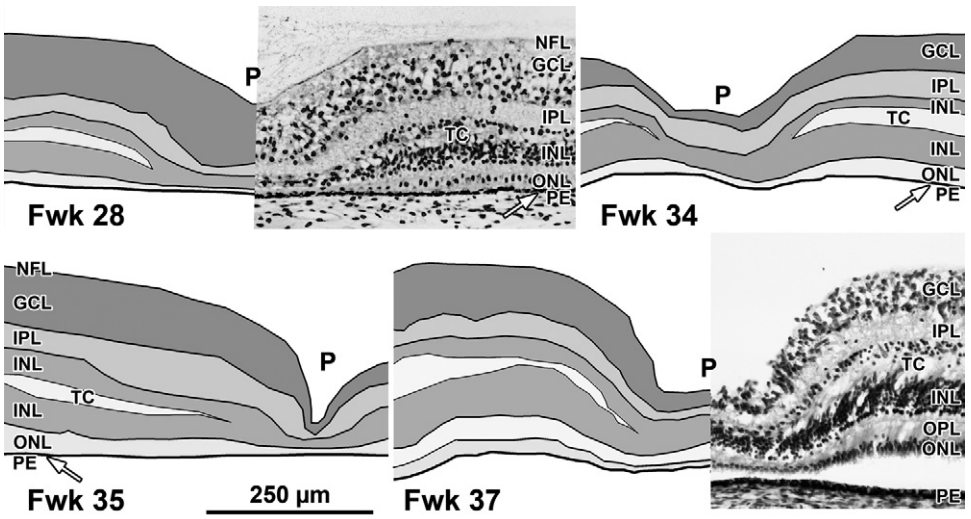

FIGURE 3. Layers of late-gestation fetal human retina. Development of the human fovea at (Top left) Fwk 28, (Top right) Fwk 34, (Bottom left) Fwk 35, and (Bottom right) Fwk 37. A transient layer of Chievitz (TC) is present as a gap in the INL of all eyes from this age group. The foveal pit (P) has thinned the GCL, IPL, and INL compared to layers surrounding the pit (the foveal slope). Scale in Bottom left for all. GCL = ganglion cell layer; INL = inner nuclear layer; IPL = inner plexiform layer; NFL = nerve fiber layer; ONL = outer nuclear layer; OPL = outer plexiform layer; PE =retinal pigment epithelium.

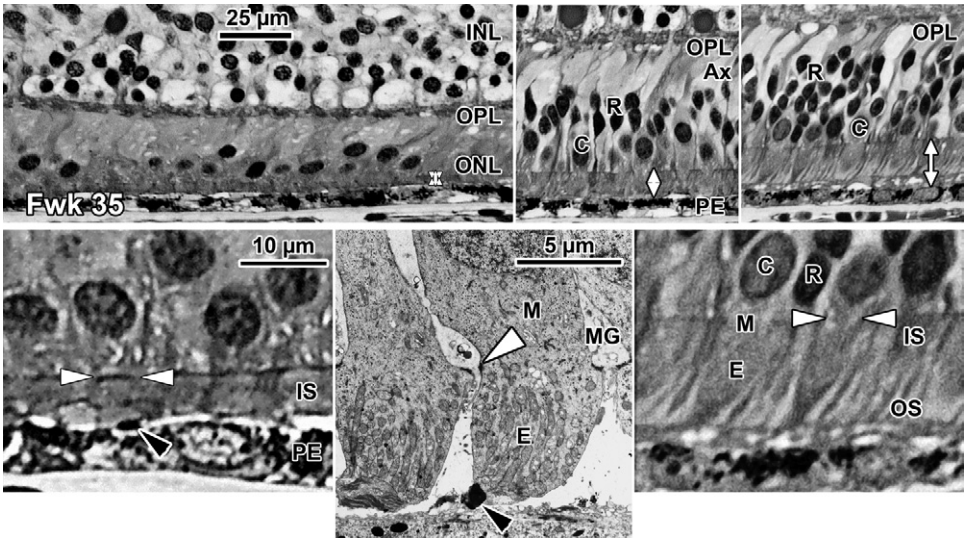

FIGURE 4. Histology of late-gestation fetal human retina. A Fwk 35 retina is shown (Top left, Bottom left), at the fovea, (Top middle) at 800 µm from the fovea where there are 2-3 layers of rods, and (Top right, Bottom right) at 2 mm from the fovea. Longer axons (Ax) are appearing on cones (C) and rods (R) outside the fovea (Top middle, Top right), which tilt away from the pit center (fovea to left). Note that the space between the ELM and PE (vertical double arrows) is widest in the periphery. Short OS are present on both rods and cones in the periphery (Top right, Bottom right) but are difficult to recognize close to or in the fovea (Bottom left, Bottom middle, black arrowhead). (Bottom middle) Two Fwk 30 foveal cones shown in a low-magnification electron micrograph. The desmosomal junctions between Müller (MG) glia and cones forming the ELM can be resolved (white arrowhead). Each cone is surrounded by pale MG cytoplasm. IS myeloid (M) and ellipsoid (E) are indicated. Scale in Top left for Top row; scale in Bottom left for Bottom row. ELM = external limiting membrane; INL = inner nuclear layer; IS = inner segment; ONL = outer nuclear layer; OPL = outer plexiform layer; OS = outer segment; PE =retinal pigment epithelium.

RESULTS

• **NORMAL ADULT RETINA:** A section from adult human retina ~2 mm nasal to the fovea is shown in Figure 1 for orientation to the layers and abbreviations used in the developing retina. A young adult fovea is shown in Figure 7 (Bottom row).

• **DEVELOPMENT OF THE HUMAN FOVEA:** *Fetal week 20–27 (11 retinas examined).* At midgestation, the future fovea had 3 distinctive differences from peripheral retina. First, the GCL is much thicker than in the periphery. Second, up to birth the ONL is formed by a single layer of cone photoreceptors (Figure 2, Bottom left; Figure 8, Top left). This is in marked contrast to the thicker peripheral ONL containing both cones and rods (Figure 2, Bottom right; Figure 8, Top middle-left and middle-right). Third, the OPL is a narrow band of cone synaptic pedicles (Figure 2, Bottom left and insert, Bottom middle; Figure 8, Top right upper panel, and Bottom). These layers will undergo developmental changes that are critical to interpreting late prenatal and neonatal SDOCT images. In the following narrative, numbers like 800 µm or 2 mm indicate distance from the fovea center.

Rods are absent across the central 1500–1800 µm, forming a region called the rod-free zone underlying the thickened GCL.[5,7] Central cones are 6–8 µm wide, with a large prominent nucleus (Figure 2, Bottom left insert; Figure 8, Top left; Figure 9, Top right lower panel). Each cone has a short axon (Ax), which ends below the cell body in a synaptic pedicle (Figure 2, Bottom left insert, arrow; Figure 8, Top middle-left); these form the thin OPL (Figure 8, Top row). Foveal cones are separated by Müller cell processes filling the space between cones. These end in small bulbs forming junctions with the cone cell bodies, creating the ELM (Figure 2, Bottom left, white arrowhead; Figure 9, Top row).

A thick short extension of cone cytoplasm, the primitive IS, can be seen distal to the ELM (Figure 2, Bottom left insert), but OS are not obvious. However, immunolabeling for opsin reveals that all central cones and rods have short OS by Fwk 25 (Figure 8, Top left to Top middle-right; also see [5,7]). Immunolabeling for synaptic proteins shows that all Fwk 20–25 cones have pedicles that contain many synaptic markers (Figure 8, Top right upper panel, and Bottom). These markers indicate that, despite their immature morphology, many of the essential molecular markers for photoreceptor function are expressed by Fwk 25.

Outside the rod-free zone, rods become much more numerous so that by 2 mm (Figure 2, Bottom right; Figure 8, Top middle-left and middle-right) the ONL is formed by a single layer of large cones and 3–4 layers of rod cell

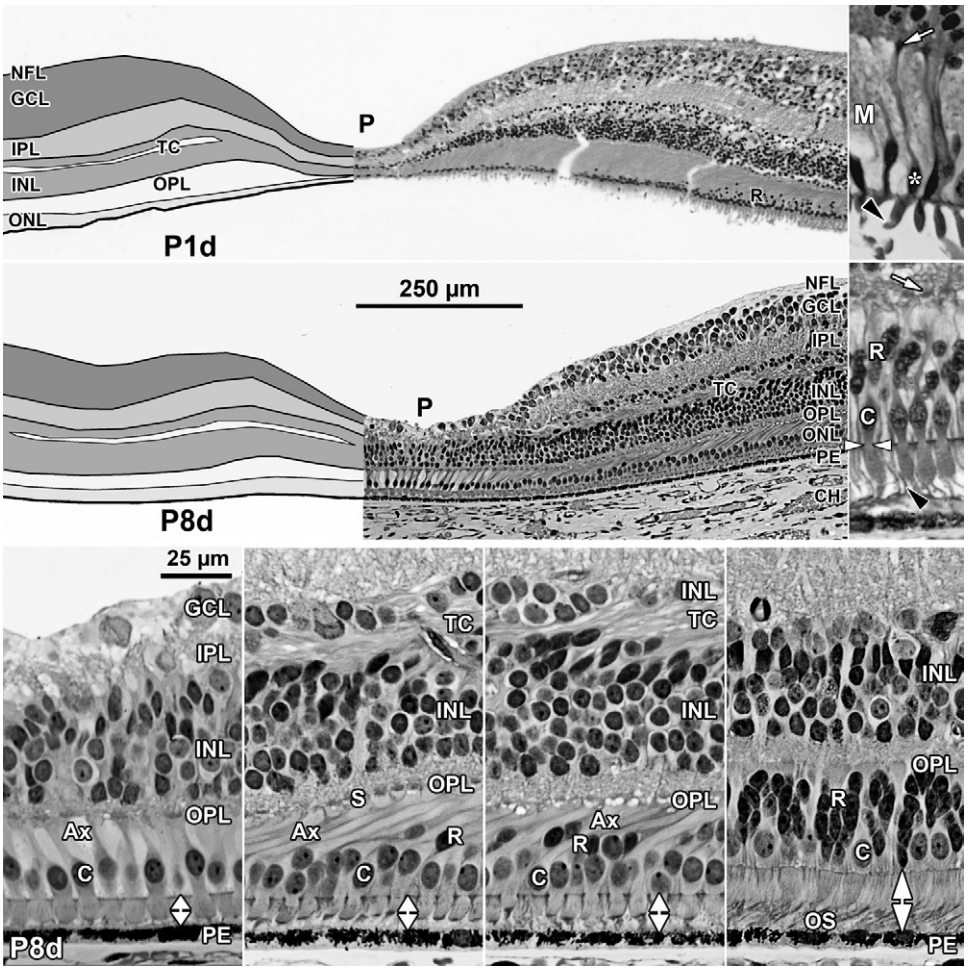

FIGURE 5. Layers and histology of postnatal-term human retina. Development of the human fovea at (Top left) postnatal (P) 1 day (d) and (Middle left) P8d. These retinas illustrate the range in development found around birth. In both retinas the pit is wider and more shallow than before birth and has displaced most of the inner layers and extends close to the cone synapses. A TC is present in the INL. Cones on the pit slope are 2-3 cell bodies deep and have long axon (Ax), but a single layer of cones still is present over the pit center. At P1d rods (R) are within 500 µm of the foveal center. (Top right) One of the cones (asterisk) on the slope from another P1d eye is shown at higher power. The IS is longer and narrower than before birth, and a short OS is present (arrowhead). The long Ax ends in a synaptic spherule (arrow). Note the large amount of pale M cytoplasm surrounding each cone, also seen around foveal cones in Middle left. (Middle right) A P8d retina at 1 mm. Both cone (C) and rod (black arrowhead) OS are obvious. P8d photoreceptors (Bottom left) at the foveal center, (Bottom middle-left) on the foveal slope at the first rods, and (Bottom middle-right) 800 µm and (Bottom right) 2 mm from the fovea. Note that the distance between ELM and PE (vertical double arrows) has increased at the fovea, but is still narrower than in the periphery. OS are present at all locations but are much shorter in the fovea compared to the periphery. The fibrous acellular nature of the TC can be seen in Bottom middle-left and middle-right. Scale in Middle left for Top and Middle left; scale in Bottom left for all others. CH = choroid; ELM = external limiting membrane; GCL = ganglion cell layer; INL = inner nuclear layer; IPL = inner plexiform layer; IS = inner segment; OS = outer segment; NFL = nerve fiber layer; ONL = outer nuclear layer; OPL = outer plexiform layer; PE =retinal pigment epithelium; TC = transient layer of Chievitz.

bodies. The rod cell bodies are added between the cone nuclei and pedicles, causing cone axons to lengthen. Paradoxically, both cone and rod IS are longer at 2 mm than in the fovea (compare Figure 2, Bottom left and right).

In most Fwk 25–27 eyes (Figure 2, Top right and Middle right) the inner layers are displaced peripherally to form a shallow foveal pit (P). The exception was a Fwk 27 fovea (Figure 2, Middle left), which had a prominent doming of all layers into the vitreous and a small detachment of the cones from the PE. No pit could be detected in multiple serial sections of this eye.

Fetal week 28–37 (8 eyes examined). All retinas had a distinct foveal pit with an outward displacement of the GCL, IPL, and INL, although the pit varied in width, depth, and layers involved. On the pit edges ("slope") the INL becomes divided by a layer of pale fibers and/or cytoplasm, which

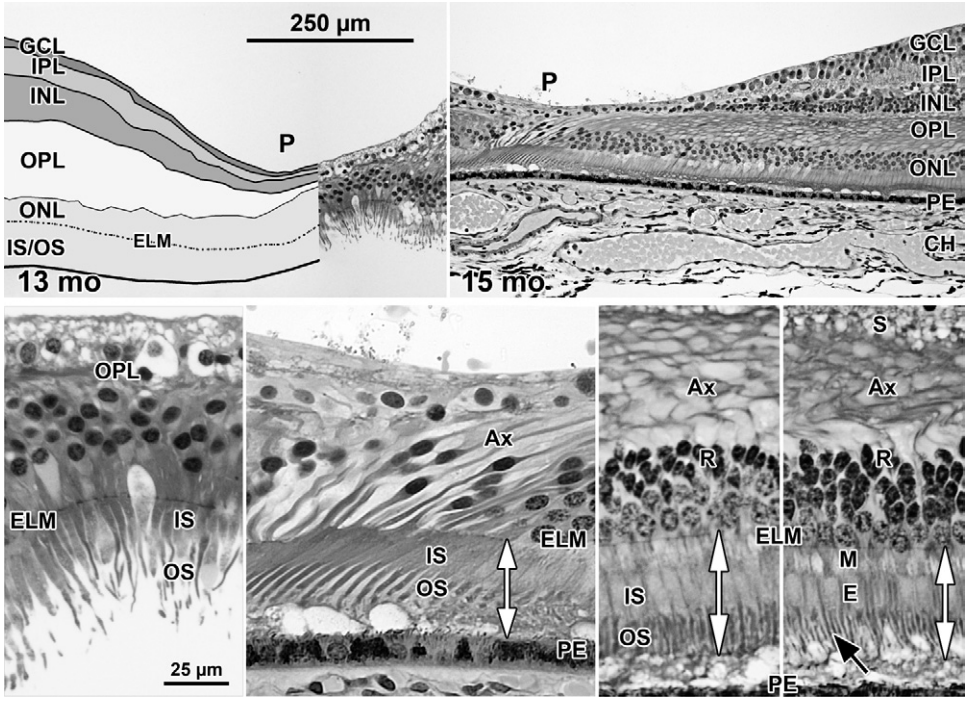

FIGURE 6. Layers and histology of human retina during infancy. Postnatal maturation of the human fovea at (Top left) 13 months and (Top right) 15 months. Over the early postnatal months, the pit becomes wide and shallow with almost no neurons in the center except cone cell bodies. The drawing in Top left illustrates the large postnatal growth in thickness of the OPL, mainly attributable to the increased number and length of cone axon (Ax). (Bottom left) Note the increase in ONL cone cell bodies over the 13 months pit center attributable to postnatal cone packing. These have long thin IS and OS. At 15 months, by comparing the double vertical arrows, it can be seen that (Bottom middle-left) foveal IS/OS, and IS/OS on photoreceptors at (Bottom middle-right) 800 µm and (Bottom right) 2 mm from the fovea now are similar in length. Long thin rod OS (Bottom right, black arrow) are prominent outside of the foveal center. Cone synapses (S) are absent from the foveal center (Bottom left and middle-left) because they have been displaced onto the pit slope (Bottom right, S). Scale in Top left for Top row; scale in Bottom left for Bottom row. CH = choroid; ELM = external limiting membrane; GCL = ganglion cell layer; INL = inner nuclear layer; IPL = inner plexiform layer; IS = inner segment; OS = outer segment; ONL = outer nuclear layer; OPL = outer plexiform layer; PE =retinal pigment epithelium.

separates the innermost cell bodies from the remainder of the INL. This layer is the transient layer of Chievitz (TC), a common feature in primate retinas around birth.[5,9,20] Immunocytochemical labeling indicates that the TC fibers are mainly Müller cell processes (Figure 9, Bottom row), which angle away from the foveal pit, reflecting the displacement of neurons and glia peripherally as the pit forms.

Up to birth the foveal cones still form a single layer under the developing pit (Figure 3). Cones are more tapered and the vertical axis of cones on the pit slope is tilted with the apical IS end pointing toward center and the synaptic axon and pedicle pointing away (Figure 4, Top row). This tilt and INL thinning indicates that the neurons postsynaptic to the foveal cones are being displaced peripherally by pit formation. The space between the ELM and RPE is still only ~5 µm wide in the fovea (Figure 4, Top left, vertical double arrows). Foveal OS can be identified but are extremely short (Figure 4 Bottom left and middle, arrowhead). Peripheral to the foveal center (Figure 4, Top middle and right) the ONL now has 2–6 deeper layers of rod cell bodies. Axons form on the foveal cones and rods on the pit slope (Figure 4, Top middle) to maintain their synaptic contacts as pit formation forces inner neurons away from the fovea. This is reflected in the axon tilt away from the photoreceptor cell bodies (Figure 4, Top right, pit center to left).

The space between the ELM and PE is 12.5 µm at 800 µm (Figure 4, Top middle, white vertical arrow) and 20 µm at 2 mm (Figure 4, Top right, white vertical arrow). Peripheral rods and cones have tapered IS and short OS, which are clearly more developed than on foveal cones (compare Figure 4, Bottom left and right).

The rod-free zone is narrower, with rods present ~600 µm from the pit center. This suggests that cone packing has started,[11,14] although cones remain in a single layer across the central retina up to birth.

Postnatal 1 day - 6 weeks (6 retinas examined). The pit becomes deeper and wider after birth with the INL, IPL, and GCL only 1–2 cells deep (Figure 5, Top left). A TC is still present in the INL in some retinas, even those well fixed by histologic criteria. Over the pit a single layer of short cones persists (Figure 5, Top right, Middle left, Bottom left; Figure 7, Bottom middle-right; Figure 8, Top

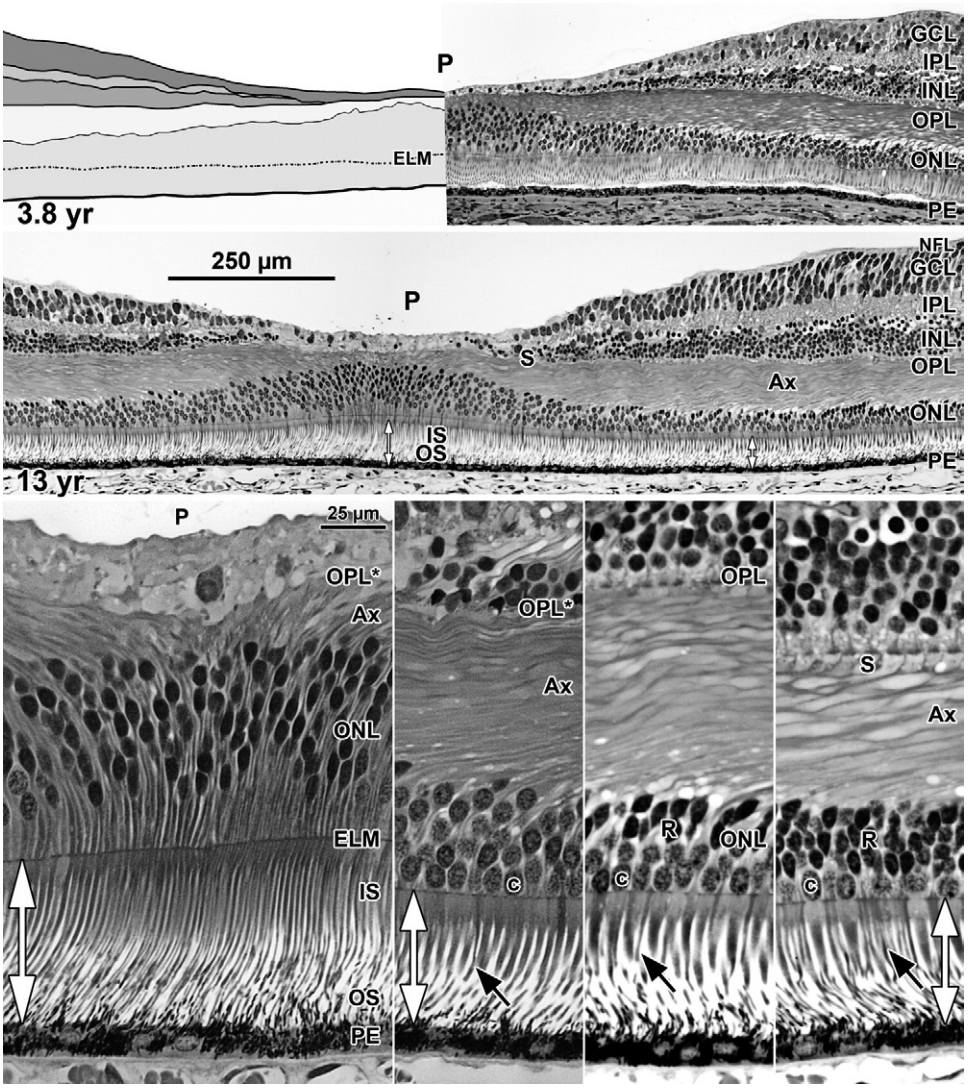

FIGURE 7. Layers and histology of human retina during childhood. The final maturation stages of the human fovea are shown at (Top left) 3.8 years (yr) and (Top right) 13 years with higher magnification of the 13 years (Middle) foveal center, (Bottom left) first rods at 300 µm, (Bottom middle-left) 500 µm, and (Bottom middle-right) 2 mm from the fovea. The foveal pit is wide and shallow. The foveal center is composed of long thin cone OS, IS, and cell bodies 8-12 cones deep. The central OPL contains a thick layer of axon (Ax). The foveal OPL contains only Ax (OPL*) out to 500 µm, where synaptic pedicles (Bottom middle-left, OPL; Bottom middle and far right, S) are first encountered. Long thin rod OS (Bottom row, black arrows) become more prominent with eccentricity. Note the marked increase in cone IS diameter from the foveal center to 300 µm with a small further increase at 2 mm. Scale in Middle for Top and Middle rows; scale in Bottom left for Bottom row. ELM = external limiting membrane; GCL = ganglion cell layer; INL = inner nuclear layer; IPL = inner plexiform layer; IS = inner segment; OS = outer segment; NFL = nerve fiber layer; ONL = outer nuclear layer; OPL = outer plexiform layer; PE =retinal pigment epithelium.

right upper panel), but slope cones are thinner, elongated, and packed into 2-3 layers (Figure 5, Middle right). Changes in the OPL in and around the fovea are striking after birth. Long cone axons are prominent across central retina (Figure 5, Bottom left to middle-right; Figure 8, Middle center and Middle right), making the OPL a much thicker layer. Most cones are angled with their cell bodies closer to the pit center than their synaptic axons and pedicles (Figure 5, Bottom middle-left and middle-right, pit center to left). Central cones (Figure 5, Bottom left and Bottom middle-left) have elongated tapered IS and short OS (Figure 5, Bottom left, white vertical arrow), but peripheral IS and OS still are longer than foveal. The gap between ELM and PE is 14 µm in the fovea and 20 µm at 1 mm (Figure 5, Bottom middle-right) and 30 µm at 2 mm (Figure 5, Bottom right) from the fovea.

In this age group the 2 postnatal 1 day retinas and 1 postnatal 8 days retina were morphologically more mature than the other P8d retina (compare Figure 5, Top left and Middle left). This may illustrate the expected variability

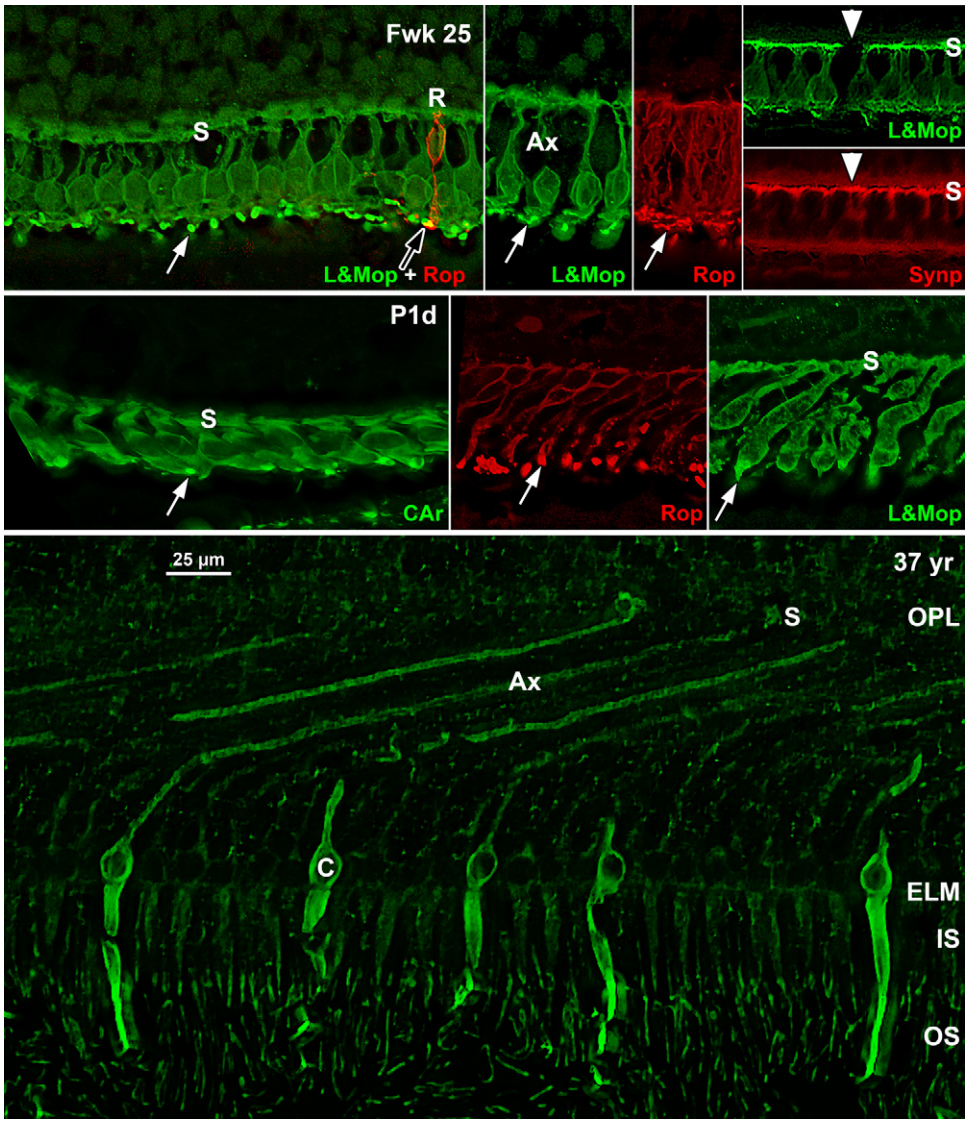

FIGURE 8. Immunocytochemistry of photoreceptor maturation. (Top row) Human Fwk 24-25 retina immunocytochemically labeled for rod opsin (red) and cone L&M opsin (green). The entire cone and rod membrane are labeled at this age, outlining the cell shape. (Top left) Each foveal cone has a short vertical axon ending in a row of synaptic pedicles (S) forming the OPL. A short cone OS is indicated by the white arrow. A single rod (R) with a tiny OS (black arrow) is on the edge of the fovea. (Top middle-left and middle-right) Photoreceptors at 2 mm from the fovea. Note the longer OS (arrows). (Top right) Foveal cones stained for L&M opsin (green; upper panel) and synaptophysin (red; lower panel), a synaptic vesicle marker. The synaptic pedicle (S) is labeled in all L&M cones and in 1 short-wavelength-selective cone (white arrowhead) unlabeled for L&M opsin. (Middle row) Postnatal 1 day (P1d) retina showing the change in photoreceptor morphology from the (Middle left) foveal cones to (Middle center) rods and (Middle right) cones 800 µm from the fovea. The foveal cones are short and relatively flat while the peripheral photoreceptors have axons tilted away from the foveal center. Note the difference in length between foveal and peripheral OS (arrows). (Bottom) A 37-year-old (37 yr) retina at 1 mm labeled for short-wavelength-selective cone opsin. The cone on the left can be traced from OS to synaptic pedicle (S). The striking change in central cone morphology from midgestation to adult can be appreciated by comparing Bottom to Top middle-left. Scale in Bottom for all. Ax = axon; ELM = external limiting membrane; IS = inner segment; OS = outer segment; OPL = outer plexiform layer.

both at birth and in postnatal development. The 5-week retina had increased growth in central IS and OS but in other respects resembled the postnatal 1 day retina.

Nine to 15 months (3 retinas examined). In 2 of the 3 retinas, in the pit center the GCL, IPL, and INL have fused into a single thin layer (Figure 6, Top right). The pit is wider than at earlier ages. Foveal cones are packed 2–4 nuclei deep and have thin, long IS and OS (Figure 6, Bottom left and Bottom middle-left). The axons on foveal cones further elongate as cone packing into the fovea occurs after birth. Long axons are prominent across central retina (Figure 6, Top right, Bottom middle-left, and Bottom right). This formation and elongation of photore-

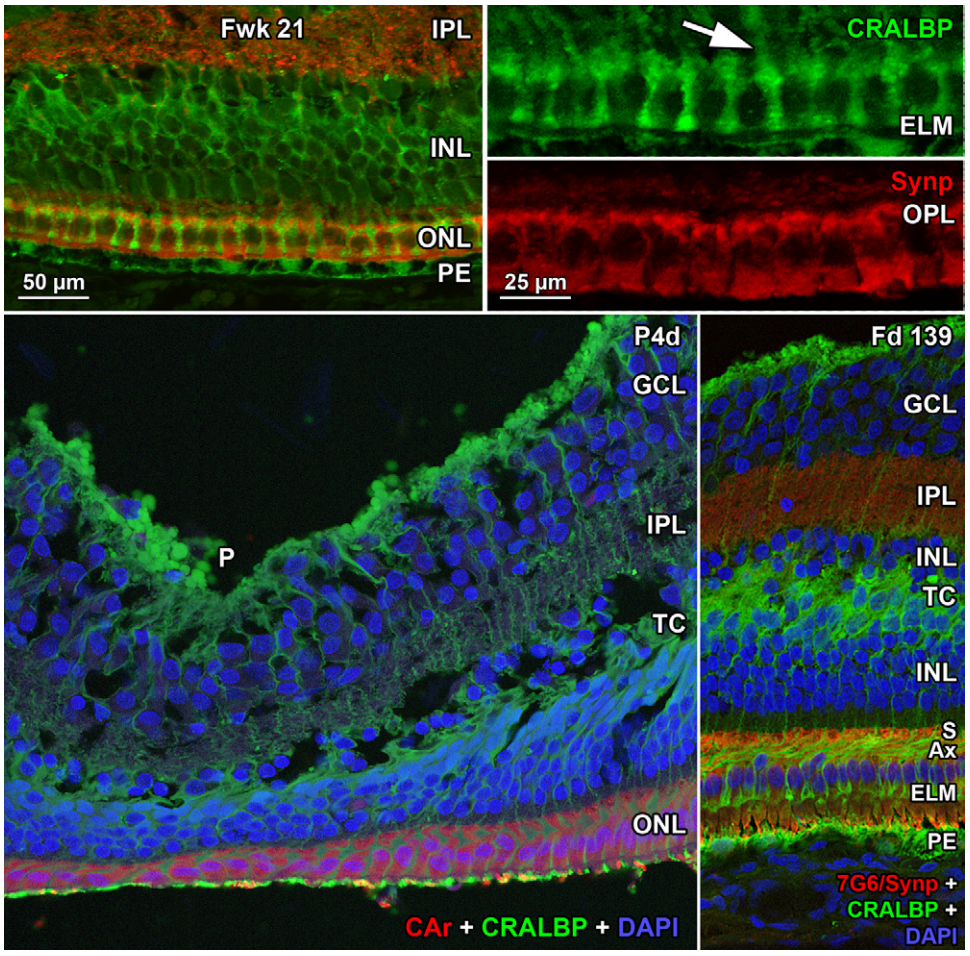

FIGURE 9. Immunocytochemistry of Müller cell morphology. (Top row) Fwk 21 fovea immunocytochemically labeled for the Müller cell protein CRALBP (green) and synaptophysin (red). Müller cell processes extend from the cell body deep in the INL, run between each cone (Top right upper panel, arrow), and form small clubs at the ELM. In the fovea Müller cytoplasm fills all space between foveal cones. (Bottom left) Postnatal 4 day (P4d) fovea triple labeled for cone arrestin (red), CRALBP (green), and nuclear label DAPI (blue). Cones over the pit (P) are in a thin single layer, but are longer on the slope. The TC is filled with Müller processes. (Bottom right) The foveal slope from a late prenatal Macaca monkey fetus triple-labeled for a mixture of cone transducin and synaptophysin (red), CRALBP (green), and nuclear label DAPI (blue). This retina more clearly shows the glial fiber makeup of the TC. Note how the Müller cell processes follow the angle of the cone axons (Ax) and then turn 90 degrees to run between the cones to form the ELM. Scale in Top left for Top left and Bottom row; in Top right for Top right upper and lower panels. ELM = external limiting membrane; GCL = ganglion cell layer; INL = inner nuclear layer; IPL = inner plexiform layer; NFL = nerve fiber layer; ONL = outer nuclear layer; OPL = outer plexiform layer; PE =retinal pigment epithelium; TC = transient layer of Chievitz.

ceptor axons around the fovea eventually makes the OPL a combination of a thick layer of axons and a single layer of cone synaptic pedicles. The OPL around the fovea is much thicker than in the periphery, where it contains mainly synaptic contacts (Figure 1). In the first postnatal year, synaptic pedicles are disappearing over the pit (compare Figure 6 Bottom middle-left to Bottom right) as all INL neurons are displaced peripherally. Eventually these cellular migrations eliminate the OPL entirely from the foveal center (Figure 7, Top and Middle). For the first time, in this age group foveal and peripheral IS and OS are similar in length (compare double arrows in Figure 6 Bottom middle-left to Bottom right). In the postnatal 13 months specimen with a detached retina, foveal IS/OS are up to 46 µm long while slope cones are 36 µm long.

These changes around 12 months indicate that pit formation is nearing its close, that cones are still packing into the foveal center, and that foveal IS and OS are elongating compared to peripheral.

Twenty-eight months to 13 years (5 retinas examined): The pit becomes wider and more shallow by 3.8 years (Figure 7, Top left), with virtually no neurons left in the > pit center except cone cell bodies ~8 bodies deep. Foveal IS are much thinner than slope IS and OS are

longer. The 3.8-year fovea is morphologically similar to that at 13 years but has not completed cone packing, as indicated by its cone density of 108 400/mm^2, compared to 208 200/mm^2 for a 37-year-old adult.[10]

At 13 years (Figure 7, Middle) the fovea appears mature in all aspects. Cone cell bodies in the foveal ONL are up to 12 bodies deep, and the floor of the pit contains Müller cytoplasm, cone axons, and the occasional neuron. Foveal cone IS are very thin and so tightly packed that it is difficult to discern single IS. There is a marked IS width gradient from foveal center to IS at 2 mm (compare Figure 7, Bottom row). The IS shape is also different, being almost straight in the fovea and tapered in the rest of the retina. Foveal cone IS are 168–189 μm long and ~3 μm wide throughout their length, while OS are 139–155 μm long. At the first rods (~300 μm) cone IS are 92–105 μm long and ~6 μm wide with OS 126 μm long. At 2 mm OS are ~40 μm long, almost 4× shorter than foveal OS.

DISCUSSION

THIS STUDY SHOWS THE PRONOUNCED CHANGE IN HUMAN foveal morphology in both the inner and outer layers of the retina from midgestation to early adulthood. Because assignment of layers is critical to SDOCT interpretation,[18,19] understanding these qualitative and quantitative changes allows us to establish a standard reference for pediatric SDOCT. This correlation is presented in a corresponding article.[20] The second point that emerges is the marked similarity in human foveal development compared to Old World *Macaca* and New World marmoset monkeys.[12,21–24] Human late fetal and infant necropsy retinas are scarce, especially with maximal preservation, which allows detailed analysis of cellular development. There also is a marked similarity between adult monkey and human in SDOCT/histology.[25] This allows us to draw inferences about human development from well-preserved monkey fetal and infant retinas of known age. It also suggests that research into neonatal development vs SDOCT images would be feasible in monkeys.

This study documents the marked changes that occur within the central human retina after midgestation. Starting at Fwk 25, outward displacements of the inner retinal layers begin to form the foveal pit. Molecular analysis of the macular region beginning at Fwk 8 indicates the presence of axon guidance molecules such as pigment epithelium–derived factor, natriuretic peptide precursor B, collagen type IV alpha 2, and ephrin A6.[26,27] These factors probably act first to repel axons and later blood vessels to form the foveal avascular zone.[21,28–30] Pit formation begins shortly after Fwk 24–25 when the foveal avascular zone is formed.[30] Modeling and quantitative morphology[15,16,31] underscore the importance of the foveal avascular zone in pit development, with intraocular pressure acting on it to initiate invagination. By 13–15 months, pit formation appears complete, with a single, broken layer of neurons in the pit center.

This paper documents the dramatic changes in the outer retina that mainly occur after birth. The foveal ONL contains a single layer of cones until after birth but then attains a 10–12 cone cell body deep thickness by 6–8 years.[9,32,33] Cone elongation and packing are mainly postnatal events, and it is just this period in which the pit shape changes from narrow and deep to wide and shallow, presumably because of retinal stretch during eye growth.[16] Cone density is 18 472 cones/mm^2 at Fwk 22 before a pit is apparent, doubles to 36 294 at birth when the pit is narrow, rises to 52 787 at 15 months, and at 108 439 cones/mm^2 is within the bottom end of the adult range at 3.8 years.[10] Thus pit remodeling may influence early phases of cone packing,[16,34] but the cause for doubling of density between 15 months and 3.8 years is not obvious. A correlation of fibroblast growth factor expression and cone packing has been described,[35] but its exact role is unclear.

Of direct interest to SDOCT imaging is the observation that from Fwk 22 to birth foveal cones have short, thick IS and very short OS while cones at 1–2 mm have longer IS and OS. This pattern was verified in vivo through 3-dimensional mapping of premature infant photoreceptor OS on SDOCT volumes.[19] This was first shown by Bach and Seefelder,[32] who provided the first description of human foveal development, and has been noted subsequently for monkeys[8,15,21] and humans.[9,33,36] This pattern is unexpected in that all descriptions of expression of opsin, synaptic proteins, and other photoreceptor molecules in humans[2,5–7,37] find expression first in and around the fovea, with a subsequent progression into the periphery. Thus photoreceptor differentiation begins very early in the fovea, but further maturation is delayed until well after birth.

At birth peripheral cone IS/OS are twice as long as foveal, by 15 months foveal and peripheral IS/OS are about the same length, and by 13 years foveal OS are 4× longer than at 2 mm. IS and OS growth might be suppressed to facilitate cone displacement into the fovea. However, cone density rises 1.5× between birth and 15 months when elongation begins, and then doubles between 15 months and 13 years when it finishes,[10] demonstrating that very long IS and OS do not inhibit most cone packing.

An additional change within the outer retina is the postnatal elongation of cone and central rod axons. This changes the OPL from a thin layer of synaptic terminals to a layer as thick as or thicker than the ONL. Photoreceptor axons are formed as a result of neuronal displacements in foveal development.[8,13,24] Foveal photoreceptors form synapses before midgestation[37] (Figure 8, Top right) with INL neurons. As these neurons are displaced peripherally by pit formation, photoreceptor axons elongate to keep contact. Axons must elongate further after birth when photoreceptors are displaced centrally to raise cone density. Thus

photoreceptor axons form to retain synaptic integrity during these 2 opposing neuronal movements.

This paper expands the existing literature and shows that the human fovea develops over a very long period. Morphologically the incipient fovea can be identified at Fwk 11–12 by its characteristic lamination. In the last half of gestation the pit forms by GCL, IPL, and INL displacement, which is finished by 1–2 years. Foveal cones change little in late gestation, but in the first year after birth they become elongated cells with long IS, OS, and axons, and by 4–6 years they develop the longest IS and OS in the retina. Concurrently, cones are packed into the fovea to raise cone density 10×. These processes are completed before 10 years when the fovea has its adult characteristics.

Now that technical advances in SDOCT imaging have made it possible to study prenatal and neonatal human eyes, the data presented here will be critical in interpreting clinical images of retinal microstructures in young infants. These histologic data provide a reference of normal development that will aid in the diagnosis of abnormal development detected in SDOCT imaging.

ALL AUTHORS HAVE COMPLETED AND SUBMITTED THE ICMJE FORM FOR DISCLOSURE OF POTENTIAL CONFLICTS OF Interest. Cynthia A. Toth receives royalties through her university from Alcon, and obtained research support for other studies from Bioptigen, Genentech, and Physical Sciences Inc. Publication of this article was supported by the Heed Ophthalmic Foundation, Cleveland, Ohio (L.V.). This research was made possible by the following grants: The Hartwell Foundation Biomedical Research Award, Memphis, Tennessee (C.A.T.); NIH Core Grants for Vision Research EY5722 and EY01730, Bethesda, Maryland; Research to Prevent Blindness (RPB) Unrestricted Grant to Washington University, and RPB Physician Scientist Award, New York, New York (C.A.T.). Involved in conception and design (A.H., C.A.T.); analysis and Interpretation of the data (A.H., D.P., L.V., C.A.T.); writing the article (A.H., C.A.T.); critical revision of the article (A.H., D.P., L.V., C.A.T.); final approval of the article (A.H., C.A.T.); data collection (A.H., D.P.); and provision of materials, patients, or resources (A.H., C.A.T.). Postmortem specimens were obtained under University of Washington Human Subjects Approval #010447.

REFERENCES

1. Seiler MJ, Aramant RB. Photoreceptor and glial markers in human embryonic retina and in human embryonic retinal transplants to rat retina. *Brain Res Dev Brain Res* 1994;80(1-2):81–95.
2. Nag TC, Wadhwa S. Expression of GABA in the fetal, postnatal, and adult human retinas: an immunohistochemical study. *Vis Neurosci* 1997;14(3):425–432.
3. Nag TC, Wadhwa S. Developmental expression of calretinin immunoreactivity in the human retina and a comparison with two other EF-hand calcium binding proteins. *Neuroscience* 1999;91(1):41–50.
4. Milam AH, Hendrickson AE, Xiao M, et al. Localization of tubby-like protein 1 in developing and adult human retinas. *Invest Ophthalmol Vis Sci* 2000;41(8):2352–2356.
5. Xiao M, Hendrickson A. Spatial and temporal expression of short, long/medium, or both opsins in human fetal cones. *J Comp Neurol* 2000;425(4):545–559.
6. O'Brien KM, Schulte D, Hendrickson AE. Expression of photoreceptor-associated molecules during human fetal eye development. *Mol Vis* 2003;9:401–409.
7. Hendrickson A, Bumsted-O'Brien K, Natoli R, Ramamurthy V, Possin D, Provis J. Rod photoreceptor differentiation in fetal and infant human retina. *Exp Eye Res* 2008;87(5):415–426.
8. Hendrickson A, Kupfer C. The histogenesis of the fovea in the macaque monkey. *Invest Ophthalmol Vis Sci* 976;15(9):746–756.
9. Hendrickson AE, Yuodelis C. The morphological development of the human fovea. *Ophthalmology* 1984;91(6):603–612.
10. Yuodelis C, Hendrickson A. A qualitative and quantitative analysis of the human fovea during development. *Vision Res* 1986;26(6):847–855.
11. Diaz-Araya C, Provis JM. Evidence of photoreceptor migration during early foveal development: a quantitative analysis of human fetal retinae. *Vis Neurosci* 1992;8(6):505–514.
12. Hendrickson A. A morphological comparison of foveal development in man and monkey. *Eye (Lond)* 1992;6(2):136–144.
13. Packer O, Hendrickson AE, Curcio CA. Development redistribution of photoreceptors across the Macaca nemestrina (pigtail macaque) retina. *J Comp Neurol* 1990;298(4):472–493.
14. Robinson SR, Hendrickson A. Shifting relationships between photoreceptors and pigment epithelial cells in monkey retina: implications for the development of retinal topography. *Vis Neurosci* 1995;12(4):767–778.
15. Springer AD, Hendrickson AE. Development of the primate area of high acuity. 2. Quantitative morphological changes associated with retinal and pars plana growth. *Vis Neurosci* 2004;21(5):775–790.
16. Springer AD, Hendrickson AE. Development of the primate area of high acuity, 3: temporal relationships between pit formation, retinal elongation and cone packing. *Vis Neurosci* 2005;22(2):171–185.
17. Springer AD, Troilo D, Possin D, Hendrickson AE. Foveal cone density shows a rapid postnatal maturation in the marmoset monkey. *Vis Neurosci* 2011;28(6):473–484.
18. Spaide RF, Curcio CA. Anatomical correlates to the bands seen in the outer retina by optical coherence tomography: literature review and model. *Retina* 2011;31(8):1609–1619.
19. Maldonado RS, O'Connell RV, Sarin N, et al. Dynamics of human foveal development after premature birth. *Ophthalmology* 2011;118(12):2315–2325.
20. Vajzovic L, Hendrickson A, O'Connell R, et al. Maturation of the human fovea: correlation of spectral domain optical coherence tomography findings with histology. *Am J Ophthalmol* 2012. Forthcoming.
21. Hendrickson A, Troilo D, Possin D, Springer A. Development of the neural retina and its vasculature in the marmoset Callithrix jacchus. *J Comp Neurol* 2006;497(2):270–286.

22. Curcio CA, Hendrickson A. Organization and development of the primate photoreceptor mosaic. In: Osborne N, Chader J, eds. Progress in Retinal Research. Oxford: Pergamon Press; 1991:89–120.
23. Provis JM, Diaz CM, Dreher B. Ontogeny of the primate fovea: a central issue in retinal development. *Prog Neurobiol* 1998;54(5):549–580.
24. Hendrickson A, Provis J. Comparison of development of the primate fovea centralis with peripheral retina. In: Sernagor E, ed. Retinal Development. Cambridge: Cambridge University Press; 2006:126–149.
25. Anger EM, Unterhuber A, Hermann B, et al. Ultrahigh resolution optical coherence tomography of the monkey fovea. Identification of retinal sublayers by correlation with semithin histology sections. *Exp Eye Res* 2004;78(6):1117–1125.
26. Kozulin P, Natoli R, O'Brien KM, Madigan MC, Provis JM. Differential expression of anti-angiogenic factors and guidance genes in the developing macula. *Mol Vis* 2009;15:45–59.
27. Kozulin P, Natoli R, Madigan MC, O'Brien KM, Provis JM. Gradients of Eph-A6 expression in primate retina suggest roles in both vascular and axon guidance. *Mol Vis* 2009;15:2649–2662.
28. Gariano RF, Iruela-Arispe ML, Hendrickson AE. Vascular development in primate retina: comparison of laminar plexus formation in monkey and human. *Invest Ophthalmol Vis Sci* 1994;35(9):3442–3455.
29. Provis JM, Sandercoe T, Hendrickson AE. Astrocytes and blood vessels define the foveal rim during primate retinal development. *Invest Ophthalmol Vis Sci* 2000;41(10):2827–2836.
30. Provis JM, Hendrickson AE. The foveal avascular region of developing human retina. *Arch Ophthalmol* 2008;126(4):507–511.
31. Springer AD, Hendrickson AE. Development of the primate area of high acuity. 1. Use of finite element analysis models to identify mechanical variables affecting pit formation. *Vis Neurosci* 2004;21(1):53–62.
32. Bach L, Seefelder R. Atlas zur entwicklungsgeschichte des menschlichen auges. Leipzig: W. Engelmann; 1914:1–148.
33. Abramov I, Gordon J, Hendrickson A, Hainline L, Dobson V, LaBossiere E. The retina of the newborn human infant. *Science* 1982;217(4556):265–267.
34. Springer AD. New role for the primate fovea: a retinal excavation determines photoreceptor deployment and shape. *Vis Neurosci* 1999;16(4):629–636.
35. Cornish EE, Natoli RC, Hendrickson A, Provis JM. Differential distribution of fibroblast growth factor receptors (FGFRs) on foveal cones: FGFR-4 is an early marker of cone photoreceptors. *Mol Vis* 2004;10:1–14.
36. Hendrickson A, Drucker D. The development of parafoveal and mid-peripheral human retina. *Behav Brain Res* 1992;49(1):21–31.
37. Nag TC, Wadhwa S. Differential expression of syntaxin-1 and synaptophysin in the developing and adult human retina. *J Biosci* 2001;26(2):179–191.

Biosketch

Anita Hendrickson, PhD, is Professor Emerita of Ophthalmology and Biological Structure, University of Washington, Seattle, Washington. She has published 175 peer-reviewed papers and reviews on primate brain and retinal development. Her work on primate foveal structure and development has been recognized by the Paul Kayser International Award of Merit in Retina Research (1998), Proctor Medal from Association for Research in Vision and Ophthalmology (2002), and University Distinguished Faculty Lecturer in Medicine (2004).

Biosketch

Cynthia A. Toth, Professor of Ophthalmology and Biomedical Engineering at Duke University (Durham, North Carolina), is a clinician-scientist, vitreoretinal surgeon. She directs the Duke Advanced Research in SDOCT Imaging Laboratory (DARSI Lab). Her translational research interests include ophthalmic diagnostics outside of conventional clinical settings, microsurgical instrumentation, and novel imaging biomarkers to improve the diagnosis, treatment, and outcomes for adults and children with vitreoretinal disease.